Full Length Article

Experimental and theoretical methods for evaluating ash properties of pine and El Cerrejon coal used in co-firing

P. Xing [a], L.I. Darvell [a], J.M. Jones [a,*], L. Ma [b], M. Pourkashanian [b], A. Williams [a]

[a] Energy Research Institute, School of Chemical and Process Engineering, University of Leeds, Leeds LS2 9JT, UK
[b] Energy Technology and Innovation Initiative, University of Leeds, Leeds LS2 9JT, UK

HIGHLIGHTS

- Reliability of XRF analysis of fuel ashes improved by wet chemical analysis.
- Ash melting behaviour of different coal-pine blends assessed via laboratory methods.
- Indices and viscosity models tested for El Cerrajon-Pine blends.
- Thermodynamic modelling usefully predicts slag formation.

GRAPHICAL ABSTRACT
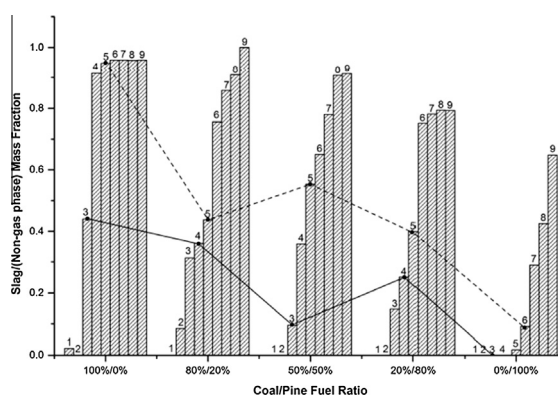
ARTICLE INFO

ABSTRACT

There has been an increase in the use of biomass for power generation by means of co-firing with coal as well as by the combustion of 100% biomass. Despite the advantages of biomass in reducing carbon emissions from the electricity sector, the co-firing of high percentages of biomass can potentially aggravate ash related problems in the boiler. In order to develop mitigation strategies for the formation of deposits, an understanding of the ash behaviour during the combustion of high percentages of biomass is required. In this work, ash samples from El Cerrejon coal and pine biomass were characterised for their inorganic composition by X-ray fluorescence and wet chemical methods. Relationships between these two methods were found. Furthermore, the melting behaviour of ashes from pure coal, pine, and their blends were studied through ash fusion tests (AFT) and via a method using a simultaneous thermal analyser coupled to mass spectrometer (STA-MS) for the evolved gas analysis. Pine ash has lower slagging potential than El Cerrejon coal ash and results show that for 20:80 and 80:20 pine:coal ash belends the characteristic ash fusion temperatures increase with increasing pine ash content. There is unusually higher slagging potential (lower ash fusion temperatures) at a 50:50 blend ratio. Viscosity models produced sensible results for coal and coal/pine blends, but further refinement is required for modelling the viscosity of pure biomass ash. Thermodynamic modelling of slag formation was undertaken using the FactSage model. This model was successful in predicting the changes of gas, solid and liquid phases during pure pine, coal and co-combustion.

1. Introduction

To reduce the use of fossil fuels and to help meet emission targets for CO_2 and, it is now common practice to burn 100% biomass or to co-fire with coal for the large scale generation of electricity using pulverised fuel combustion. Biomass combustion is also advantageous in many cases in terms of lowering SOx and NOx compared to using coal. However, biomass is not an ideal alternative to coal using current technologies, because of the differences in physical and chemical characteristics. The nature of the inorganic content of biomass results in ash particles which may adhere on the heat transfer surfaces, accumulate on the inside walls of the burners to form deposits or slags, and also induce boiler fouling in the convective pass. Alkali metals present may lower the melting temperature of the ash [1,2] but this is also dependent on the other metal oxides present particularly calcium. Generally, slagging takes place in the hottest parts of the boiler whilst fouling deposits occur as the flue gases and ash particles cool down [3]. Several approaches have been taken to study the formation and chemistry of these deposits. Vassilev et al. [4] used optical microscopy, X-ray diffraction (XRD) and Differential Thermal Analysis-Thermogravimetric analysis (DTA-TGA) to examine ash formation and behaviour during biomass heating and identified several steps associated with different temperature ranges: (i) fragmentation of particles <500 °C; (ii) agglomeration: initial (700–900 °C), significant (700–1100 °C) and extensive (700–1300 °C); (iii) ash melting: initial (700 °C), extensive (900–1100 °C) and complete (1100–1500 °C); (iv) phase crystallization between 500 and 1500 °C; and (v) glass liquid formation between 700 and 1500 °C.

There has been some success in relating biomass ash behaviour to the nature of the inorganic components. In this approach, the inorganics are classified into four types: (i) water soluble salts, (ii) elements associated with the inorganic fraction of the biomass, (iii) minerals included in the fuel structure, (iv) inorganic material incorporated within the biomass from extraneous sources. Removal of the water-soluble salts (alkali chlorides, sulphates, etc.) has been shown to increase the ash melting temperature in many agricultural residues and straws [5], and also to reduce fouling by alkali salts. Washing also impacts on the combustion behaviour of the fuel. In a previous study [6], water-washed and demineralised (acid wash) biomass samples were investigated to determine the effect of potassium on their devolatilisation behaviour. The influence of alkali metals on the kinetics of the thermal decomposition of biomass has also been investigated by other researchers using a similar approach [7–9]. Because of the difference in ash composition between coal and biomass, there are different classifications and amounts of inorganics present. Hence, there are possible consequences when firing blends of coal and biomass, and improvement in either char burnout behaviour and/or ash behaviour is possible. The current work examines the impact on ash behaviour.

Another approach to predicting, biomass ash behaviour and deposition tendencies is through the use of empirical coal ash indices. Under complex combustion conditions, the changes in the boiler and heat transfer passes are predicted using indices; this is a widely used approach, but their reliability when applied to coals from around the world, or when applied to blends, (coal-coal or coal-biomass) is still an issue. Also, their value is limited for biomass because there is less experience in using biomass than coal, hence validation becomes important. However, some indices have proved popular, for example the alkali index is a useful guide to fouling, and the base-to-acid ratio a guide for biomass slagging, although interpretation is different from coal [10]. These indices as well as others are evaluated in this study of pine blended with El Cerrejon coal in different ratios.

There are few reports on ash composition and deposition behaviour of El Cerrejon coal. López and Ward [11] studied the composition and mode of occurrence of mineral matter as they vary for different coal seams and also with particle size. Their studies showed that the mineral phase from El Cerrejon coal contains a high proportion of pyrite (14%) and a significant proportion of coquimbite (3.5%) on hydrated aluminium sulphate, and ~54% of quartz, and lower proportions of the clay minerals, kaolinite, and illite. The deposition behaviour of El Cerrejon coal during combustion has been studied experimentally and evaluated by a numerical simulation of its slagging propensity by Wieland et al. [10]. These authors compared El Cerrejon to Pittsburgh 8. The Watt-Fereday model (also utilised in this current study) gave reasonable prediction of deposition of El Cerrejon. The higher deposition propensity of El Cerrejon was then modelled using sticking criteria derived from a thermodynamic model (FactSage) and DTA-TGA, giving reasonable, although slightly different predictions.

Pine wood has been widely investigated for 100% combustion and also for co-firing with coal, and favourable properties have been reported [12,13]. Compared with rice husk, straw and coffee husk, pine branches shows a low ash content-with especially low SiO_2 content, but with the highest Na_2O content. Furthermore, the ash from pine resulted in higher melting and ash fusion temperatures, thereby reducing their slagging propensity. During the large-scale co-firing tests pine also showed a different behaviour from other biomass, as it resulted in a low degree of adherence to furnace surfaces.

Co-firing adds further complexity to ash behaviour because of possible interactions; these interactions are studied in this work. For example, vapour phase inorganics from the biomass ash, particularly, potassium salts, interact and react in both the gas phase and also with coal char and ash particles. These interactions take place at high temperature and can result in surface layers potassium-alumina silicate on the coal fly ash [14]. Alternatively, the coal ash can act as surface for deposition of aerosols of potassium salts. In fact, some authors have studied the addition of coal pulverised fly-ash to biomass boilers to mitigate fouling by potassium salts [15]. In this paper the ash behaviour of two fuels, El Cerrejon coal and pine, are examined in as well as blends of the two which might be used for co-firing. For this purpose, the inorganic composition of the fuels are characterised by both X-ray Fluorescence and wet chemical methods and the results obtained by both methods compared. The ash melting behaviour and ash fusion temperatures of the ash from the coal and pine and their ash blends are determined using the characteristic temperatures SST (shrinkage starting temperature), DT (deformation temperature), HT (hemisphere temperature) and FT (flow temperature) previously described [16,17]. The results are also verified with simultaneous thermal analysis coupled to a mass spectrometer for evolved gas analysis (STA-MS). This work is an expansion of earlier work [17] and uses thermodynamic modelling of slag formation in different ratios of coal and pine via the FactSage software package. Factsage has previously been used successfully to model the behaviour of coal and biomass [18,19]. The modelling results obtained here are compared with the experimental data obtained from the ash fusion tests and thermal analyses.

2. Experimental methods

2.1. Sample preparation

Ash was prepared from the pine wood and El Cerrejon coal samples according to the British Standard DD CEN/TS 15370-1:2006 and BS 1016-104.4:1998, respectively. Each sample was ashed in air at two final temperatures, namely 550 °C and 800 °C for 14 h

in a Carbolite MFS furnace. Blends of ash from these two fuels were studied. Two strategies were employed for studying ash blends from El Cerrejon coal and pine wood. The first involved ashing the fuels separately at 550 °C, as described above, followed by blending of the ashes at set mass ratios. These are termed 'ash blends' and were prepared by mixing the pine ash and El Cerrejon coal ash in proportions equivalent to (fuel) pine/coal ratios of 80/20, 50/50 and 20/80. The second strategy involved blending the fuels at mass ratios of 80/20, 50/50 and 20/80 prior to ashing at 550 °C. These are termed 'blended fuel ash'. Sample designations and ashing temperatures are given in Table 1. For the experimental analyses and tests, all the ash samples were manually sieved to a particle size <106 μm and then kept in sealed plastic containers. It should be noted that, because of the difference in ash contents in pine versus El Cerrejon coal, the ash ratios differ compared to the fuel ratios and the former are also given in Table 1.

2.2. Proximate and ultimate analyses

The proximate and ultimate analyses are presented in Table 2. The moisture, volatile and ash contents of the pine and coal were determined following British Standard methods as described before [16,17]. The fixed carbon was estimated by difference. The C, H, N, S contents were determined using a Flash EA 1112 series analyzer as well as by the analytical facilities in the School of Chemistry at the University of Leeds, where the S and Cl contents of the fuels were also analysed by wet chemical methods. The oxygen contents were determined by difference. The proximate and ultimate analyses were carried out in duplicate and the average values are reported. The high heating value (HHV) of the pine wood and El Cerrejon coal samples were calculated from their elemental contents on a dry basis using Eqs. (1) and (2) respectively, which were derived by Friedl et al. [20] and Majumder et al. [21]:

$$HHV = 3.55C^2 - 232C - 2230H + 51.2C \times H + 131N + 20600 \ (kJ/kg) \tag{1}$$

$$HHV = -0.03Ash - 0.11Moisture + 0.33Volatile + 0.35Fixed\ carbon\ (MJ/kg) \tag{2}$$

2.3. Ash analyses

The ash compositions were determined by both wet chemical analyses (WCA) and X-ray fluorescence (XRF). For the wet chemical analyses some of the major elements in the ash were measured using digestion followed by spectrophotometric determination (i.e. SiO_2, and P_2O_5). For the SiO_2 analyses, the digestate was first reacted with ammonium molybdate and the adsorption at 650 nm compared to a set of standard solutions by using a Jenway 6300 Spectrophotometer. Similarly, P_2O_5 was determined by a

reaction of the digestate with molybdovanadate solution, and the absorption at 430 nm was then compared to a set of standard solutions. Other metals such as Fe, Al, Mg, K, Na, Mn and Ti were determined by atomic absorption spectrometry (AAS) using a VARIAN AA240FS spectrometer, after the ash had been digested sequentially in HF, HCl, H_2SO_4 and HNO_3. Calcium was determined by titration with EDTA. The analysis results for the elements are reported as oxides in this paper. For the XRF analyses, the major elements in the ash samples were analysed using an ARL Advant XP Sequencial X-ray fluorescence spectrometer.

Ash fusion tests were performed using a Carbolite digital ash fusion furnace, which has a black and white camera fixed at the front of the furnace to capture images of the ash whilst it is heated at a controlled temperature rate. An ash paste was prepared from the ash samples according to British standards, as described in DD CEN/TS 15370-1:2006. The ash paste was then pressed into an upright cylindrical stainless steel mold (about 5 mm diameter and ~5 mm height). The mold was coated beforehand with an extremely thin layer of petroleum jelly to facilitate the removal of the test piece. Ash test pieces were then heated to 1700 °C at a heating rate of 5 °C/min. Images were collected by the camera for every degree of temperature rise between 555 °C and 1700 °C. These tests were performed in an oxidizing atmosphere (air). For a few samples the tests were repeated in a reducing atmosphere (50% mixture of CO/CO_2). In both cases the gas flow rates were 50 ml/min.

Ash samples were also analysed by using a Netzsch 449C Jupiter Simultaneous Thermal Analyser (STA), coupled to a Netzsch QMS 403C Aeolos Quadrupole Mass Spectrometer. Simultaneous thermal analysis involves the simultaneous application of thermogravimetry (TG), which measures sample mass loss in a controlled temperature programme, and differential thermal analysis (DTA), which monitors the temperature difference between

Table 2
Fuel properties (wt% basis).

Wt%	Pine	El Cerrejon coal
% Moisture, a.r	7.73	6.63
% Ash, a.r.	1.67	3.83
% Fixed Carbon, a.r.	17.96	41.55
% Volatile matter, a.r	72.64	47.99
% C daf	50.29	75.94
% H daf	5.74	4.26
% N daf	0.61	1.76
% S daf	0.48	0.64
% Cl daf	<0.3	<0.3
% O* daf	42.88	17.40
[a,b]HHV MJ/kg d.b.	19.46	28.63

* By difference.
[a] Pine: Calculated by Eq. (1).
[b] Coal: Calculated by Eq. (2); All measurements were in duplicate, and averages are reported.

Table 1
Ash sample designations and preparation conditions.

Sample name	Ashes (wt%)	Temperature of preparation (°C)	Ash ratio Pine:Coal
PCC1	100%El Cerrejon coal ash	550	0:100
PCC2	100%El Cerrejon coal ash	800	0:100
PPA1	100%Pine ash	550	100:0
PPA2	100%Pine ash	800	100:0
CA82	Pine ash and Coal ash at fuel ratio of 80%/20%	550	63:37
CA55	Pine ash and Coal ash at fuel ratio of 50%/50%	550	30:70
CA28	Pine ash and Coal ash at fuel ratio of 20%/80%	550	10:90
BFPC82	Blended fuels at 80%Pine/20% Coal, then ashed	550	63:37
BFPC55	Blended fuels at 50%Pine/50% Coal, then ashed	550	30:70
BFPC28	Blended fuels at 20%Pine/80% Coal, then ashed	550	10:90

the sample and an inert reference material. For these tests approx. 10 mg of ash was heated from room temperature to 1400 °C at 10 °C/min under a gas flow rate of 80 ml/min of 12.5% O_2 in He. The volatile species and gases evolved were transferred directly into the electron impact ion source of the MS via a heated fused silica capillary. The mass-to-charge ratios (m/z) of the monitored gas species were H_2O (m/z 18), C (m/z 12), CO (m/z 28), CO_2 (m/z 44), K (m/z 39), Cl (m/z 35), SO_2 (m/z 64) and KCl (m/z 74).

The ash compositions of the samples were used to calculate different slagging and fouling indices, as follows:

The alkali index was calculated from the quantity of alkali oxides in the fuel per unit of fuel energy (kg alkali/GJ) as given in Eq. (3):

$$AI = \frac{K_2O + Na_2O}{HHV} \quad (kg/GJ) \tag{3}$$

When the alkali index values are in the range 0.17–0.34 kg/GJ fouling or slagging is considered probable, when these values are >0.34 which indicates that fouling or slagging is virtually certain to occur [22].

For bituminous coal ashes, the base-to-acid ratio is also an indicator of deposition tendency [23] and can be calculated by the following equation:

$$R_{b/a} = \frac{Fe_2O_3 + CaO + MgO + K_2O + Na_2O}{SiO_2 + TiO_2 + Al_2O_3} \tag{4}$$

where each oxide is represented by the mass fraction in the ash (%). As $R_{b/a}$ increases, the fouling tendency of a fuel ash increases. When $R_{b/a} < 0.5$, the fuel shows a low slagging propensity, if $0.5 < R_{b/a} < 1.0$, the fuel shows a medium slagging propensity; when $R_{b/a} > 1.0$, the slagging propensity of the fuel is very high. Eq. (4) was originally developed for use with bituminous coals not biomass. There has been some success in the prediction of slag formation with the use of $R_{b/a}$ or just base percentage for biomass. In a study by Li et al. [24], this equation was used to evaluate biomass ash slagging tendency, and $R_{b/a}$ has some reciprocal effect on the deformation temperature. Consequently this equation has been chosen to predict the ash slagging potential from biomass, coal and their blends in this study. The reliability of $R_{b/a}$ for biomass ash and blends will be compared with other methods.

According to McLennen et al. [25], the slagging index (F_S) is based on the initial deformation temperature (DT) and hemisphere temperature (HT) observed during ash fusion tests, which has also been employed in this investigation to analyse the slagging propensity of the ash samples. The index is defined as:

$$F_S = \frac{4DT + HT}{5} \quad (°C) \tag{5}$$

In this approach, an ash is classified as having a boiler slagging propensity which is low when $F_S > 1343$ °C; medium when $1232 °C < F_S < 1343 °C$; high when $1149 °C < F_S < 1232 °C$; and severe when $F_S < 1149$ °C.

With regards to coal combustion, viscosity is an important physical property that affects deposit strength in regions of high temperature (>1100 °C) and can therefore be used to determine the extent of capture and consolidation of particles on furnace walls; with high particle viscosity yielding low slagging potential [26,27]. In this study we used the redefined Watt-Fereday viscosity model for UK coal ashes as given in Eq. (6), where m and c are the slope and intercept, respectively.

$$Log(\eta) = \frac{m \times 10^7}{(T - 150)^2} + c \quad (Pas) \tag{6}$$

where $m = 0.01404294SiO_2 + 0.0100297Al_2O_3 - 0.296285$, and $c = 0.0154148SiO_2 - 0.0388047Al_2O_3 - 0.0167264Fe_2O_3 - 0.0089096CaO - 0.012932MgO + 0.04678$; T is in °C.

In previous studies from Degereji et al. [28,29], the coal numerical slagging index (Sx) was developed for predicting co-firing slagging propensity as Eq. (7):

$$Sx = \gamma / Log(\eta) \tag{7}$$

For pure biomass and coal combustion, the mass of the incoming ash (γ) can be calculated by the ash content and the heating value of the individual fuels as follows:

$$\gamma = \frac{Ash\ content\ per\ kg}{CV\ (MJ/kg)} \tag{8}$$

For co-firing, the incoming mass of ash blends and blending fuel ash can be defined by Eq. (9), where x, y, γ_c and γ_b are the ratio of the coal in the blend, the ratio of the biomass in the blend, the mass of the coal ash and the mass of the biomass ash, respectively.

$$\gamma = x\gamma_c + y\gamma_b \tag{9}$$

The viscosity at the softening temperature is defined by the modified Watt–Fereday model [26,27], as Eq. (10). The softening temperatures of both the coal (T_c) and the biomass (T_b), are defined in Eqs. (11) and (12), respectively, as follows:

$$Log(\eta) = \frac{m \cdot 10^7}{T_s^2} + c \quad (Pa\ s) \tag{10}$$

$$T_c = a(SiO_2) + b(Al_2O_3) + c(Fe_2O_3) + d(CaO) + e(MgO) + f(\alpha)] + g + 150\ °C \tag{11}$$

$$T_b = 1.81CaO\% + 4.2Al_2O_3 - 2.4K_2O\% + 5.3P_2O_5 + 1017\ °C \tag{12}$$

and the constants a–g are parameters based on the SiO_2, Al_2O_3 and Fe_2O_3 contents in the ash, as a = 92.55; b = 97.83; c = 84.52; d = 83.67; e = 81.04; f = 91.92; g = −7891.

In Eq. (10), the term T_s for blends can be calculated as follows:

$$T_s^2 = xT_c^2 + (y/k) \tag{13}$$

The factor k in Eq. (13) is calculated from the main compound percentages from Table 3 as follows:

$$k = (K_2O + TiO_2)/Fe_2O_3 \tag{14}$$

A third model was tested which was developed based on viscosity measurements on US lignite and subbituminous coal slags. The method of Streeter follows a similar procedure to that proposed by Urbain for high silica slags, and these models have been reviewed by Vargas et al. [27]. Here, viscosity is given by:

$$ln\eta = lna + lnT + \frac{10^3 \cdot b}{T} - \Delta \tag{15}$$

$$Here,\ \Delta = m \cdot T + c \tag{16}$$

where a and b are defined as:

$$b_0 = 13.8 + 39.9355\alpha - 44.049\alpha^2 \tag{17}$$

$$b_1 = 30.481 - 117.1505\alpha + 129.9978\alpha^2 \tag{18}$$

$$b_2 = -40.9429 + 234.0486\alpha - 300.04\alpha^2 \tag{19}$$

$$b_3 = 60.7619 - 153.9276\alpha + 211.1616\alpha^2 \tag{20}$$

$$b = b_0 + b_1 SiO_2 + b_2 SiO_2^2 + b_3 SiO_2^3 \tag{21}$$

$$-lna = 0.2693b + 13.9751 \tag{22}$$

α is calculated from the mole fraction of components in the ash (ratio of glass modifiers to (glass modifiers + amphoterics) see

Table 3
Oxide contents of ash from coal pine and blends (wt%). Sample designations are given in Table 1.

Sample	SiO$_2$	P$_2$O$_5$	K$_2$O	Na$_2$O	MgO	CaO	Fe$_2$O$_3$	Al$_2$O$_3$	TiO$_2$	MnO	C	H	N
[a]PCC1	41.81±0.41	0.27±0.01	0.93±0.06	1.85±0.05	1.34±0.02	4.87±0.01	12.38±0.01	21.07±0.02	1.17±0.00	0.00±0.00	0.32	0.10	0.10
[b]PCC1	41.90	0.22	0.97	1.99	1.54	5.03	14.20	23.30	1.04	856 ppm	N/A	N/A	N/A
[a]PCC2	44.69±0.02	0.34±0.01	0.96±0.04	2.30±0.02	1.40±0.12	4.59±0.44	13.34±0.05	22.44±0.38	1.69±0.01	0.00±0.00	0.19	0.00	0.00
[b]PCC2	43.30	0.23	0.86	2.47	1.56	5.14	14.80	23.10	0.99	750 ppm	N/A	N/A	N/A
[a]PPA1	3.87±0.06	11.32±0.04	16.68±0.20	1.29±0.03	4.53±0.23	48.86±0.01	0.50±0.00	1.21±0.04	0.00±0.00	0.12±0.05	7.24	0.00	0.00
[b]PPA1	1.87	11.70	22.10	1.31	6.37	50.60	0.82	0.85	506 ppm	0.16	N/A	N/A	N/A
[a]PPA2	3.33±0.04	14.43±0.07	18.66±0.26	1.60±0.08	5.96±0.03	50.74±0.20	0.43±0.00	1.14±0.02	0.00±0.00	0.11±0.03	1.97	1.10	0.00
[b]PPA2	1.98	12.30	17.80	0.99	6.90	53.00	0.79	0.52	561 ppm	0.18	N/A	N/A	N/A
[c]CA82	18.86	7.29	10.91	1.66	3.38	32.60	5.22	9.01	0.62	0.08	N/A	N/A	N/A
[c]CA55	32.40	3.64	5.69	2.00	2.34	17.91	9.48	16.05	1.18	0.04	N/A	N/A	N/A
[c]CA28	40.72	1.41	2.49	2.20	1.70	8.89	12.09	20.38	1.53	0.01	N/A	N/A	N/A
[b]BFPC82	17.40	6.79	12.8	2.07	4.46	32.80	5.96	8.19	0.49	0.16	N/A	N/A	N/A
[b]BFPC55	29.30	3.18	7.76	1.32	2.80	17.60	11.00	14.90	0.74	0.11	N/A	N/A	N/A
[b]BFPC28	37.90	1.07	2.92	1.93	1.96	8.93	13.20	19.90	0.94	956 ppm	N/A	N/A	N/A

[a] Test by wet chemical analysis.
[b] Test by XRF.
[c] By calculation.

[27] for details). From a knowledge of the value of b (SiO$_2$ is molar ratio of silica in the ash), the fuel is classified as high-silica, intermediate silica or low-silica slag. Then the values of m and c are calculated as follows from the mole fractions of components in the ash:

High-silica slags (b > 28):

$$F = SiO_2/(CaO + MgO + Na_2O + K_2O) \tag{23}$$

$$10^3 \cdot m = -1.7264 \cdot F + 8.4404 \tag{24}$$

$$c = -1.7137(10^3 \cdot m) + 0.0509 \tag{25}$$

Intermediate-silica slags (24 < b < 28):

$$F' = b \cdot (Al_2O_3 + FeO) \tag{26}$$

$$10^3 \cdot m = -1.3101 \cdot F' + 9.9279 \tag{27}$$

$$c = -2.0356(10^3 \cdot m) + 1.1094 \tag{28}$$

Low-silica slags (b < 24):

$$F'' = CaO/(CaO + MgO + Na_2O + K_2O) \tag{29}$$

$$10^3 \cdot m = -55.3649 \cdot F'' + 37.9186 \tag{30}$$

$$c = -1.8244(10^3 \cdot m) + 0.9416 \tag{31}$$

2.4. Equilibrium modelling: FactSage

Because of the limitations of the empirical indices in the prediction of slagging and fouling, an equilibrium thermochemical model, FactSage 6.4 [30], was used to predict the formation of deposits and to gain further insights into ash behaviour. This has been applied previously, with success to coal and/or biomass blends [E.g. 17–19,31,32]. The proximate and ultimate fuel data were used as inputs. The thermodynamic database was mainly taken from FACTPS and FTOxid, all ideal gas, solid and liquid solutions were calculated from the stoichiometric equations. The reactions took place at a pressure of 1 bar and the air:fuel ratio was such that each output had an oxygen content of 6 mol% O$_2$, which is typical for a combustion chamber. A temperature range from 500 to 1800 °C was chosen for the reactions between C, O, H, N, S, P, K$_2$O, Na$_2$O, SiO$_2$, CaO, Al$_2$O$_3$, Fe$_2$O$_3$, MgO, MnO, and TiO$_2$.

3. Results and discussion

3.1. Fuel and ash analyses

The proximate and ultimate analysis of pine and coal are listed in Table 2. It can be noted that the Cl and S contents are low in these two fuels and that the ash content of pine is less than half of that of the coal. The ash composition of the individual fuels and their blends, as determined by both XRF and wet chemical analyses are given in Table 3. Fig. 1 is a plot of the metal, silicon and phosphorus compositions expressed as oxides. In the case of the blends, only the ash from the fuel blends (i.e. fuels mixed prior to ashing) were examined by XRF, whilst the composition of the ash blends (i.e. mixed after ashing) were calculated based on the ash compositions of the pure fuels (as analysed by wet chemical methods) and according to the equivalent coal/biomass blend ratio. For example, for a blend of 50:50 (mass of pine/coal) the actual ash ratio is ∼30:70. Since the ash contents of pine and coal are 1.67% and 3.83%, respectively, the different ash components are calculated by 30% of the pine ash (prepared at 500 °C) and 70% of El Cerrejon coal ash (prepared at 800 °C). To study the properties of coal and pine ash during simulated co-firing, the composition of
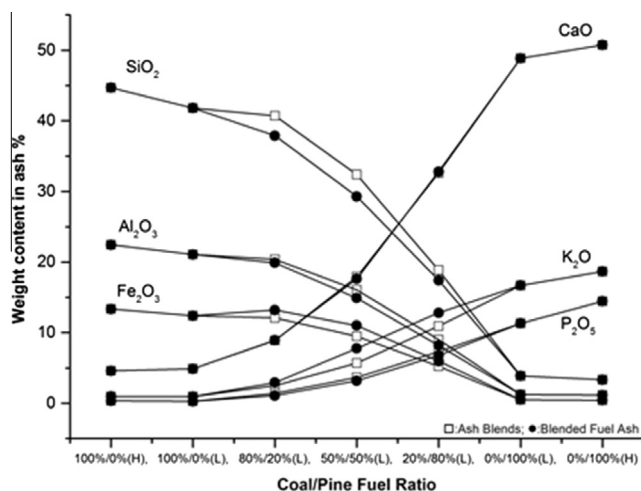
Fig. 1. Variation of major metal, silicon and phosphorus contents (expressed as oxides) for different coal/pine ratios, with ashing conditions: (H)-800 °C; (L)-550 °C.

the individual ashes prepared at both low and high temperatures were compared and some differences were observed. The high temperature ash results in lower C, H and N content, which in turn affects the proportion of inorganics (expressed as oxides) in the resultant ash analysis. Du et al. [33] used TG-DTC to study the ash from pine and a number of other biomass. They showed that laboratory ash produced at higher temperatures results in a lower yield due to decomposition and evaporation of some of the inorganic components. The ash characteristics thus vary with the preparation temperature as well as by the method of preparation. Compared with WCA, XRF has the advantage of being a rapid method of analysis, but the accuracy of this method has not been completely evaluated. In a study by Thyrel et al. [34], biomass ash components were tested by XRF. In this instance, the feasibility of using XRF results to predict reasonable results were deemed excellent, since the aluminium calibration models showed good reliability. However, when several metals are being analysed, more than one calibration will be needed, since different metals vary in their evaporation behaviour. A consequence of this is that their concentrations are affected by the fusion temperatures used to prepare the XRF sample pellets.

In order to determine the biomass ash compositions from XRF analyses, a correlation to the more accurate traditional wet chemical analysis results was developed. Agreement between the two methods was generally good with regression coefficients (R^2) > 0.9 in all cases; a database of five different reference materials (coals and biomass) enabled linear correlations to be assessed as given in Table 4. For coal ash, the XRF results for SiO_2 are compa-

rable to the wet chemical analysis. The correlations given in the equations can therefore be used as calibrations for future XRF analyses. However, this was not the case for biomass ash, where disagreement was found between the XRF results and the WCA values. The average relative deviation of different oxides for the coal and pine are shown in Table 4. For the case of pine, the errors for some of the important components are large particularly for SiO_2, Al_2O_3 MgO and K_2O. The poorest correlations found were for K_2O, MgO and CaO, meaning that there were larger errors in the analyses of biomass ash composition using XRF. These errors could be explained due to the preparation of XRF samples in a high temperature environment, which may result in some evaporation of the metals being analysed. Further work will be needed to extend the database to improve the range of the calibrations.

3.2. Ash fusion properties

The ash fusion characteristic temperatures have been listed in Table 5 for all the ash samples studied. These are plotted in Fig. 2. It can be observed that pine ash softens at temperatures between 1200 and 1500 °C, and this temperature range is higher than that observed for El Cerrejon coal ash. The melting properties of ash blends and fuel blend ashes show a similar trend: The 80:20 and 20:80 pine:coal blends show expected behaviour in that the characteristic temperatures of SST (shrinkage starting temperature), DT (deformation temperature), HT (hemisphere temperature) and FT (flow temperature) decrease as the coal ratio increases. However, in both types of blends, the 50/50 fuel ratio ash ratio gives the lowest ash fusion temperatures. These results are discussed later in the light of the FactSage computations.

The ash test pieces undergo several changes during the test, which include swelling and shrinking as discussed in Pang et al. [35]. In order to gain an insight into the behaviour of the ash during testing, the change in height of the test pieces (relative to the initial height) was estimated from the ash fusion tests images and plotted against temperature, as shown in Figs. 3–5 for the pure fuels, ash blends, and fuel blends ashes, respectively. Figs. 3–5 were generated by measuring the height of the test piece relative to the initial height, as described in [35]. It enables a classification of the different stages the test piece displays, namely Region I (no affect of heat treatment), Region II (Sintering stage where the test piece shrinks), Region III (Porous medium, where the test piece swells, which is not always present), and Region IV where there is excessive melting. Marked on the Figures are the deformation, hemisphere and flow temperatures, DT, HT and FT as determined by the standard ash fusion test. From Fig. 3 it can be observed that coal ash swells at the deformation temperature. A similar behaviour was also observed for the ash blends with coal ratios of

Table 4
Correlations and average relative deviations between wet chemical analysis (WCA) and XRF measurement of ash components.

Species	Correlation	Regression	Relative average deviation	
			Pine	El Cerrejon Coal
Al_2O_3:	$Y_{WCA} = 1.0222 X_{XRF} - 0.2417$	$R^2 = 0.9992$	0.175	0.050
Fe_2O_3:	$Y_{WCA} = 0.9789 X_{XRF} + 0.214$	$R^2 = 0.9830$	0.242	0.068
CaO:	$Y_{WCA} = 1.1816 X_{XRF} - 1.7141$	$R^2 = 0.9302$	0.017	0.016
K_2O:	$Y_{WCA} = 1.1444 X_{XRF} - 0.7094$	$R^2 = 0.9167$	0.140	0.021
MgO:	$Y_{WCA} = 1.1825 X_{XRF} - 0.2009$	$R^2 = 0.9368$	0.169	0.069
Mn_2O:	$Y_{WCA} = 1.0104 X_{XRF} + 0.0191$	$R^2 = 0.9733$	0.143	N/A
P_2O_5:	$Y_{WCA} = 0.922 X_{XRF} + 0.1933$	$R^2 = 0.9846$	0.017	0.102
SiO_2:	$Y_{WCA} = 1.027 X_{XRF} - 1.07$	$R^2 = 0.9975$	0.348	0.001

Table 5
Ash fusion characteristic temperatures and calculated slagging and fouling indices.

Samples	SST (°C)	DT (°C)	HT (°C)	FT (°C)	[a]AI	[b]B/A	[c]Fs (°C)	[d]Sx
PCC1	980	1195	1315	1330	0.04	0.33	1219	0.65
PCC2	1005	1205	1360	1375	0.04	0.33	1236	0.59
PPA1	1020	1225	1480	1510	0.15	14.16	1276	−0.38
PPA2	1085	1285	1495	1515	0.16	17.33	1327	−0.38
CA82	1170	1210	1320	1335	0.12	1.89	1232	1.02
CA55	1085	1180	1235	1250	0.09	0.75	1191	0.41
CA28	1120	1245	1290	1300	0.06	0.44	1254	0.50
BFPC82	1095	1195	1265	1295	0.14	2.23	1209	3.44
BFPC55	955	1025	1230	1245	0.10	0.90	1066	0.52
BFPC28	1075	1210	1300	1325	0.06	0.49	1228	0.57

[a] Calculated by Eq. (3).
[b] Calculated by Eq. (4).
[c] Calculated by Eq (5).
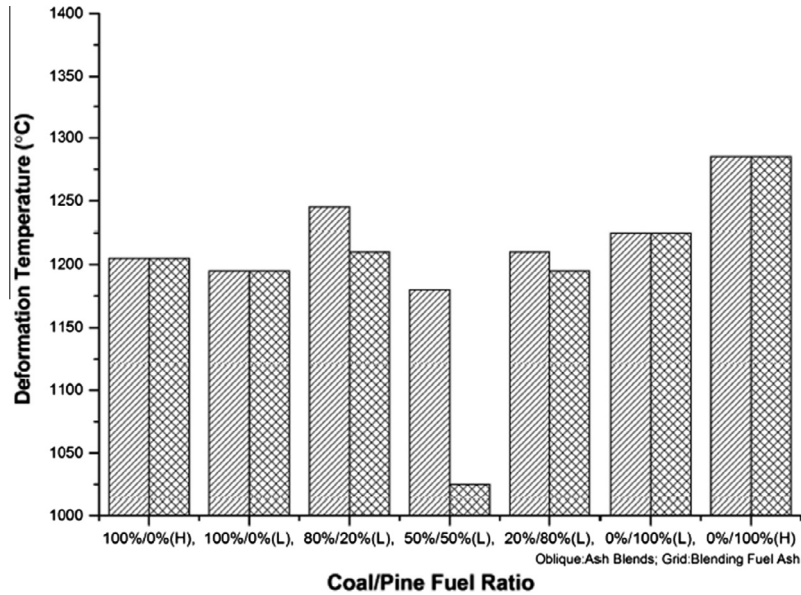[d] Calculated by Eq. (7).

Fig. 2. Plot of ash deformation temperatures with different coal/pine ratios, with ashing temperatures: (H)-800 °C; (L)-550 °C. Oblique-lined fill signifies ash produced by blending the fuels then ashing; Hatched fill signifies blended fuel ash (ash produced separatedly then blended).
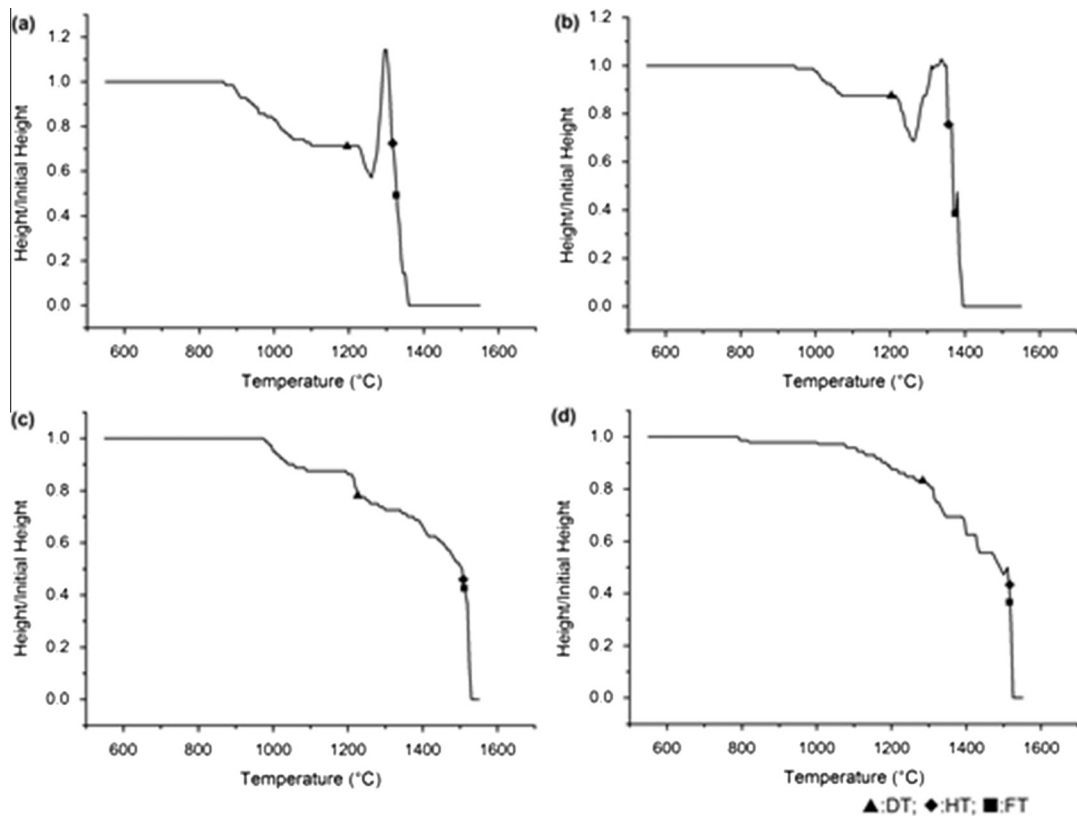

Fig. 3. Relative deformation temperatures of test samples during the ash fusion test of El Cerrejon coal ash and pine ash as a function of temperature (a) PCC1; (b) PCC2; (c) PPA1; (d) PPA2. Refer to Table 1 for sample designation.

50% or higher in Fig. 4b and c. In contrast, the pine ash, and the 80:20 blend of pine and coal, shrink at temperatures >800 °C. Moreover, the shrinking appears to accelerate upon reaching the ash fusion characteristic temperatures, as can be observed in Figs. 3c and d, and 4a. The biomass ash, which has higher K_2O and CaO contents but lower Fe_2O_3 and Al_2O_3, shrinks as the temperature increases. Since the shrinking continues until the end of

the test it is difficult to determine the swelling point with accuracy. Both ash blends and analogous blended fuel ashes behaved similarly, and their behaviours resemble that of pure coal ash as the quantity of coal in the blend increases. This can be seen clearly in Fig. 5c, when the amount of pine is <20% of the blended fuel ash, as its ash behaviour is very close to the pure coal ash behaviour, and as such it can be more confidently predicted.
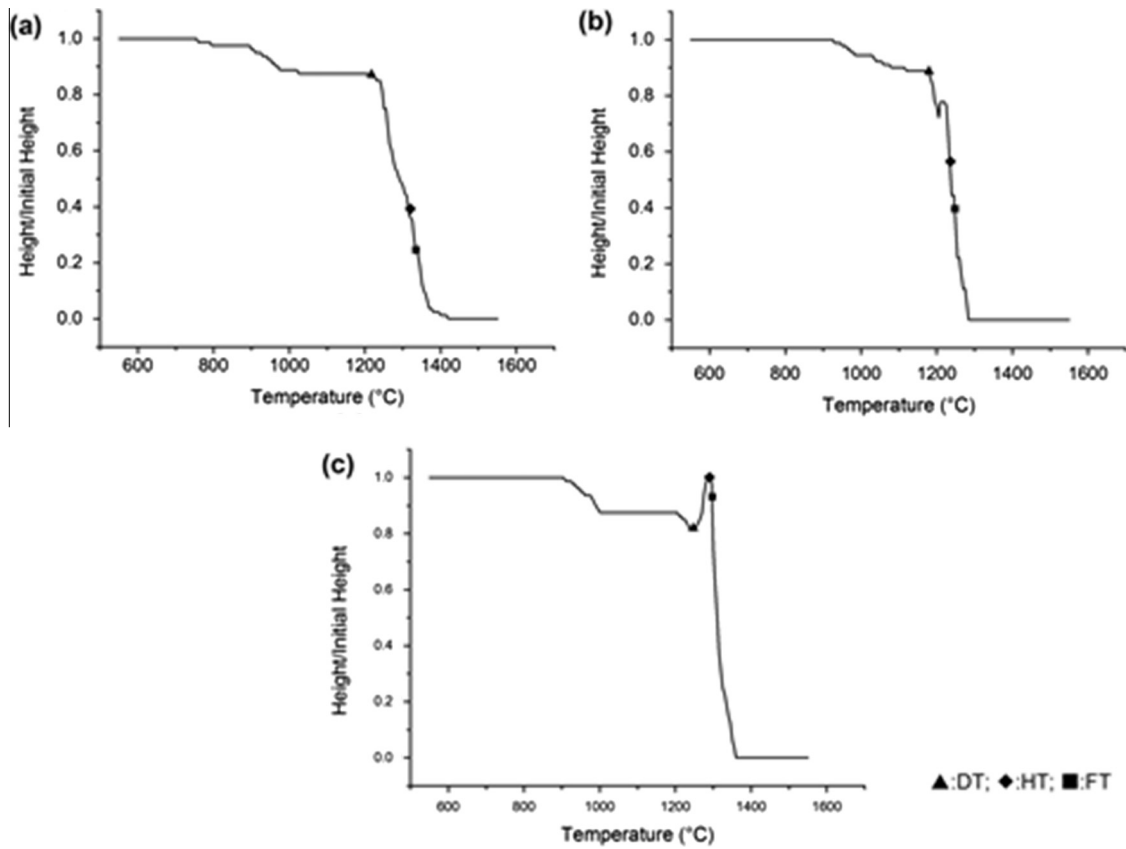
Fig. 4. Relative deformation temperatures of test samples during the ash fusion test for coal and pine ash blends: (a) CA82; (b) CA55; (c) CA28. Refer to Table 1 for sample designation.
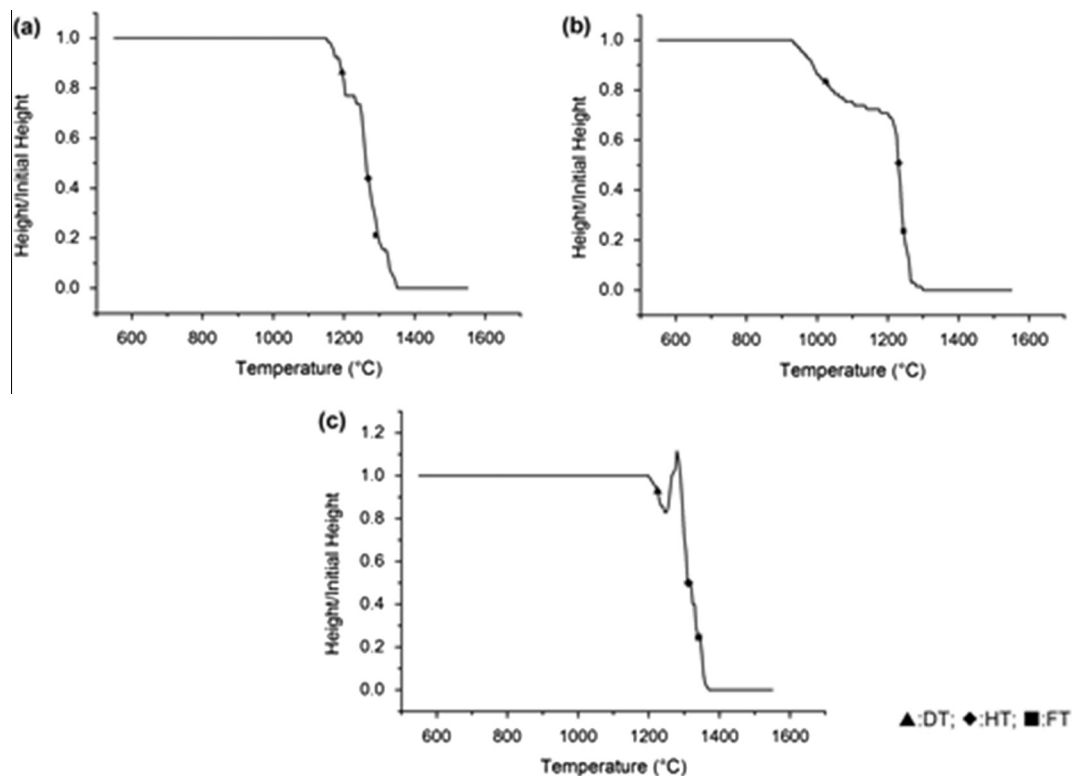

Fig. 5. Relative deformation temperatures of test samples during the ash fusion test for coal and pine blended fuel ash: (a) BFPC82; (b) BFPC55; (c) BFPC28. Refer to Table 1 for sample designation.
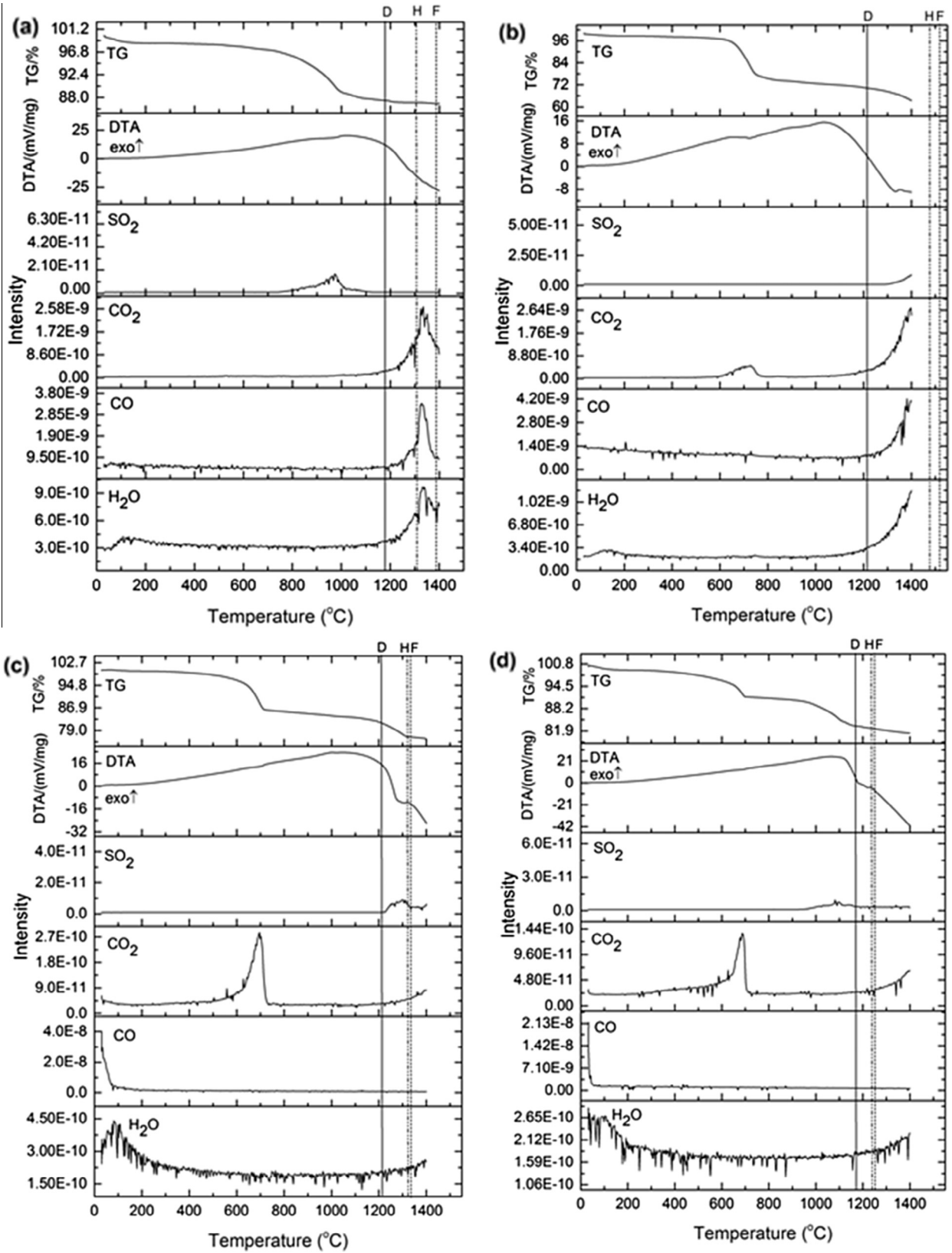
Fig. 6. Plots of mass loss, DTA and corresponding gas evolution profiles with temperature (when heated at 10 °C/min in 12.5% O_2/He) for El Cerrejon coal, pine and blended ash samples: (a) PCC1; (b) PPA1; (c) CA82; (d) CA55; (e) CA28. Refer to Table 1 for sample designation. D, H, F refer to deformation, hemisphere and flow temperatures as measured by the ash fusion test.
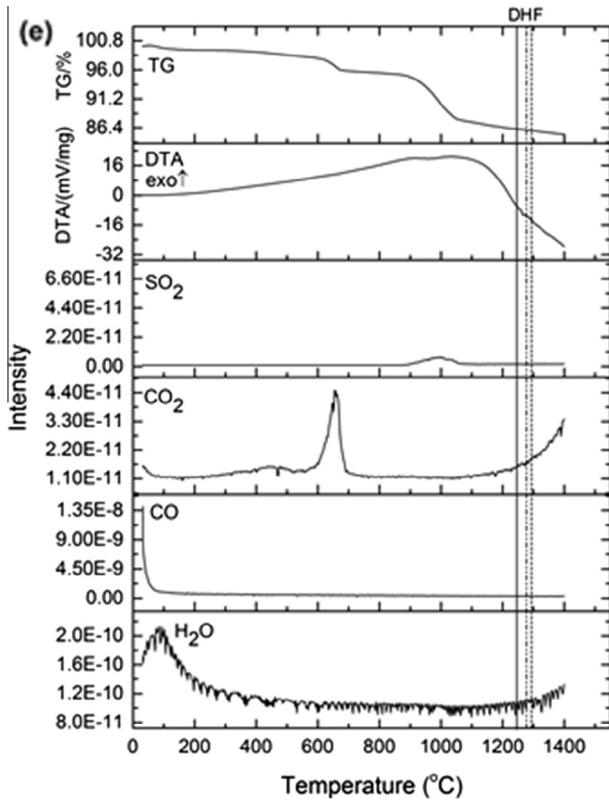
Fig. 6 (*continued*)

3.3. Melting behaviour

Plots showing the mass loss upon heating of ash samples in the STA, alongside the corresponding DTA curves and gas evolution profiles are presented in Fig. 6a–e. The mass loss curves are complex with gradual mass losses up to the final temperature of 1400 °C. Melting in the STA is characterised by the DTA curve becoming endothermic from temperatures at and above the deformation temperature. Comparisons of the endothermic portion of the DTA curve with characteristic ash fusion temperatures: deformation (DT), hemispherical (HT), and flow temperatures (FT) are marked in Fig. 6, and values are given in Table 5. In most ash samples the temperatures for the start of melting (as detected by STA) are lower than the deformation temperatures observed in the standard ash fusion test, and are closer to the SST.

Fig. 6a shows the evolution profiles for CO_2, CO, SO_2 and H_2O from the melting of the low temperature coal ash. Moreover, it can be observed that SO_2 evolves at much lower temperatures than the ash fusion deformation temperature. Similar evolution profiles were observed for the PCC2 ash (not shown), which is a high temperature ash, and as such it resulted in a lower peak intensity for SO_2 than the lower temperature ash.

For the pine ash (Fig. 6b), the ash fusion hemisphere and flow temperatures are closer and are much higher than its deformation temperature. Similar to the low temperature coal ash, the low temperature pine ash (PPA1) also shows peaks for the evolution of CO_2 and CO, which reach a maximum as the temperature approaches the deformation temperature.

Comparing the ash blends in Fig. 6c–e with the ash from the fuel blends (not shown here), the TGA and DTA curves are very similar to the PPA1 in Fig. 6b, as the ratio of pine increases, but the DT, HT, and FT are much closer together and higher than the results from the DTA curve. In general, the ash blends with high biomass ash ratio show higher fusion temperatures than the high coal ash blends. The behaviour of the 50/50 fuel ratio ash is interesting as it results in the lowest characteristic temperatures. The peak for the SO_2 emission shifts to lower temperatures as the coal ash content in the blend is increased.

Baxter et al. [16], who used the STA-MS method to characterise biomass ash, found a correlation between the ash fusion hemisphere temperature and the endotherm (DTA) peak temperatures for Miscanthus ash samples. In Fig. 7 the data from the ash and ash blends studied were plotted alongside data from Baxter et al. for comparison purposes. It can be observed that most of the ash samples studied here show higher HT values than the endothermic peak temperature estimated from the STA with the exception of the 80/20 fuel blend ash (BFPC82), for which both temperatures are close.
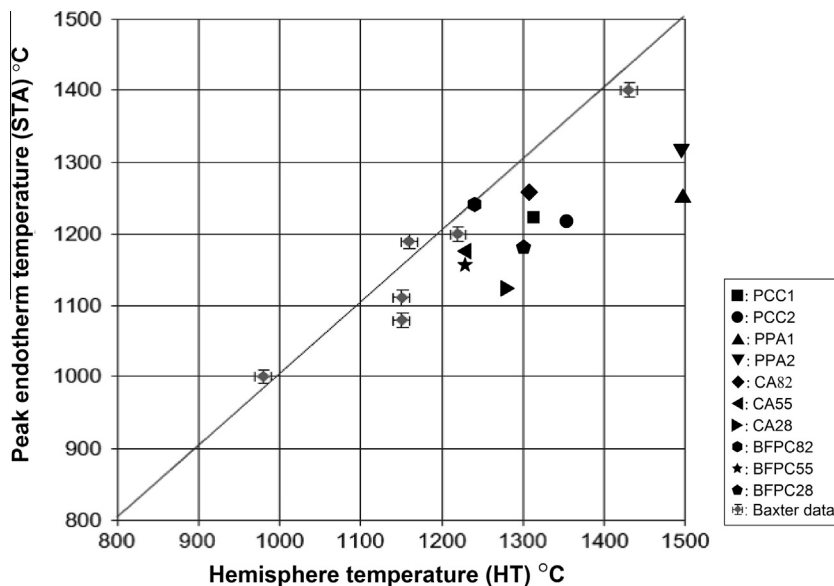

Fig. 7. Plot of experimental hemisphere temperatures (HT) and peak endotherm temperatures (STA) for various fuels compared with the results by Baxter et al. [16]
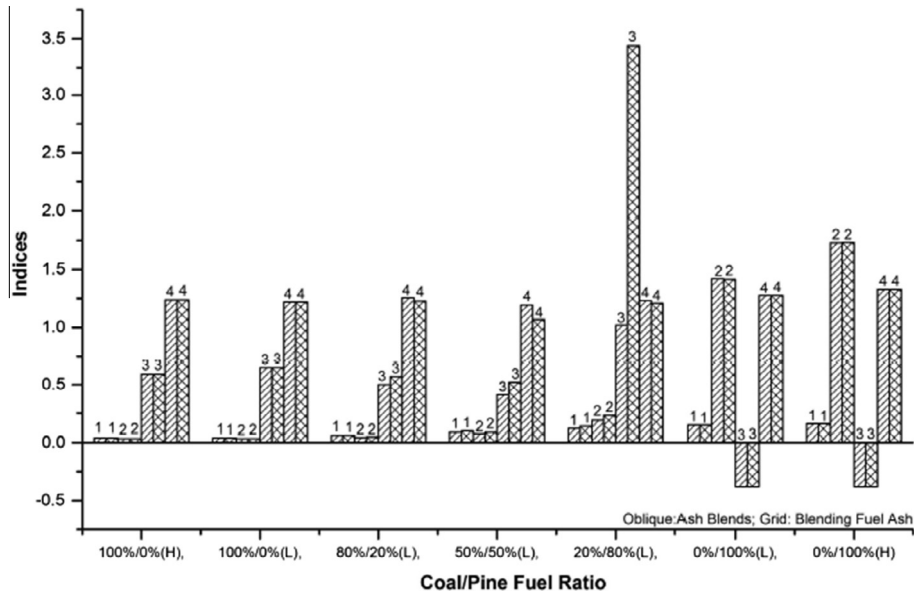
Fig. 8. Values for different numerical indices at various coal/pine ratios, with ashing temperatures: (H)-800 °C; (L)-550 °C. Indices: 1, AI kg/GJ; 2: $R_{a/b}$ x10; 3: Sx; 4: Fs/1000 (°C). Oblique-lined fill signifies ash produced by blending the fuels then ashing; Hatched fill signifies blended fuel ash (ash produced separatedly then blended).
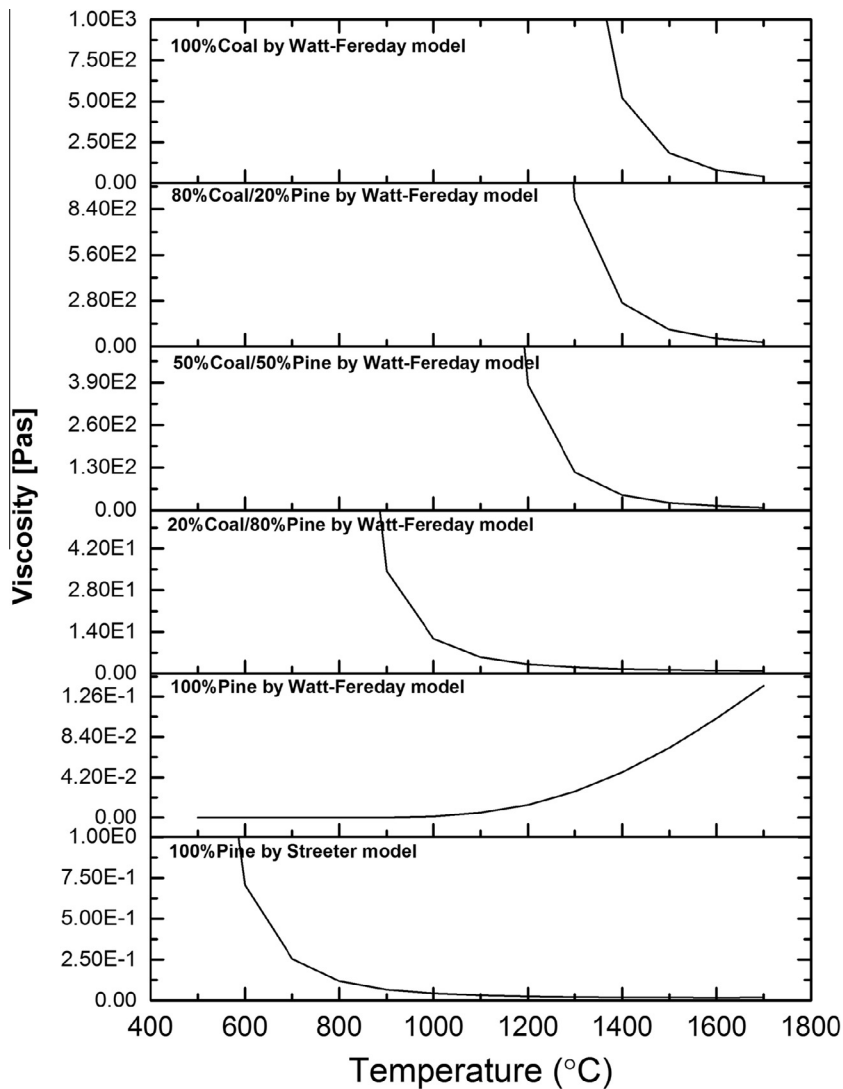

Fig. 9. The change of viscosity with temperature for ash from different fuels based on the Watt-Fereday viscosity model, calculated by Eq. (6); for comparison the Streeter model for lignite is shown, applied to the pine.

3.4. Slagging/fouling indices

Listed in Table 3 are the major components of the ash samples. The pine and El Cerrejon coal ash compositions were determined by WCA, whilst the ash compositions for the fuel blends were determined by XRF as described earlier. In the case of the ash blends, their composition was calculated from the fuel ash compositions according to their ash blending ratio. The slagging and fouling indices are listed in Table 5 and Fig. 8 is a plot of different numerical indices results with different coal/pine ratios.

The calculated AI indices for all coal/pine fuel ratios are similar for both methods of ash preparation and indicate that all the fuels studied have low fouling potential. However, the calculated base-to-acid ratio, ($R_{b/a}$), indicates that 100% pine ash a has high slagging potential, which is not observed in the ash fusion test. The low temperature coal ash PCC1 and the high temperature coal ash PCC2 show low slagging potential. For the ash blends, increasing the biomass ratio from 20 to 80% increased the ash slagging potential from low to high. In the case of the ash from the fuel blends, a similar trend was also observed with the BFPC82, which is predicted to have a high slagging propensity; increasing the coal content decreased the slagging propensity: BFPC55 shows medium slagging propensity and BFPC28 low slagging propensity.

The calculated F_S slagging indices predict that both pure pine ashes (prepared at 550 °C (PPA1) and at 800 °C (PPA2)) would have low slagging propensities. The coal ash PCC1 and PCC2 are predicted to have medium slagging potential. However, different predictions for both types of ash blends are obtained from the $R_{b/a}$, where the fuel blend ashes, CA55 and BFPC55 show a high slagging propensity according to the AFT. The other ash blends (CA82, CA28, BFPC82 and BFPC28) show high slagging potential.

The calculated values of Sx (at the shrinkage starting temperature, SST) show that because the total amount of ash decreases with the increase of biomass ratio as shown in Fig. 8, the slagging potential decreases slowly from 100% coal to 50% coal and 50% biomass. A distinctive feature is a sharp increase when the biomass is 80% of the blend. With pure biomass the value of Sx shows the lowest slagging potential based on this index. Possibly

this refects the crossover point of the Al_2O_3 and K_2O concentrations in the ash.

The variation of viscosity with temperature is illustrated in Fig. 9 for both the fuel and the blend ashes. The Watt-Fereday model predicts decreasing viscosity with increasing temperature for the coal ash, the 80:20, 50:50 and the 20:80 blend of coal and pine. It is seen that for pure coal the ash is predicted to have high viscosity up to 1400 °C, which is related to a low slagging propensity. As the percentage of pine ash in the blend increases, the temperature for slagging decreases, and it is predicted to be around 900 °C for the 20:80 coal:pine ash blend. To put the model in some context it can be compared to the glass working point viscosity (when it can be blown), which is 1000 Pa s, and the glass melting point viscosity, which is 10 Pa s. It should be noted that using this model, pine ash is predicted to have low viscosity (<0.1 Pa s) for the entire temperature range. However, the Watt-Fereday viscosity model is an empirical index based on the viscosities of UK bituminous coal ash melts and therefore needs further refinement and validation for high CaO ashes such as pine ash. In comparison, the model by Streeter was also tested for the pine ash (a low silica slag) and the results are given in Fig. 9 also. While the model does show decreasing viscosity with temperature, it predicts a highly slagging ash with exceptionally low softening temperature, which was not seen experimentally. This model was developed for lignites and sub-bituminous coals. The results here highlight the need for a more refined and validated viscosity model for biomass ashes.

3.5. Thermal equilibrium model

In order to gain understanding of the slagging and fouling processes and to be able to predict the slagging potential of the fuels, a thermal equilibrium model for the different fuels was built up using FactSage. The modelling results showing the thermal equilibrium phase changes for the ashes from pure pine, El Cerrejon coal and fuel blends with respect to the combustion temperature are presented in Fig. 10. Each bar in the chart represents the predicted mass fraction of slag for a particular blend at a particular tempera-
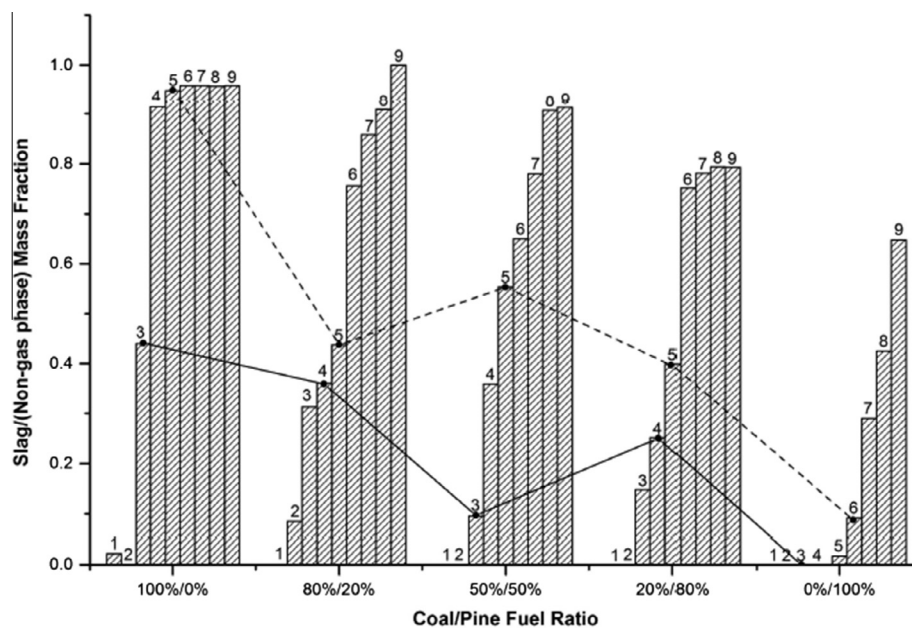

Fig. 10. The change of slag weight content (%) in non-gas phase with increase in temperature for each coal/pine ratio as calculated by FactSage. Temperatures: 1, 800 °C; 2, 900 °C; 3, 1000 °C; 4, 1100 °C; 5, 1200 °C; 6, 1300 °C; 7, 1400 °C; 8, 1500 °C; 9, 1600 °C. Solid and dashed line represents the lower and upper limits of the measured deformation temperature range (by ash fusion test) for the different blends.

ture. Also plotted on this figure are the lower and upper limits of the measured deformation temperature ranges, assumed to be represented as the lowest softening temperature (SST) and highest deformation temperature (DT) measured for each blend or pure fuel; the solid and dashed line join these points to give an estimated region for where slagging is observed to occur experimentally.

The first thing to note is that the coal is predicted to be the most slagging (i.e. has the largest change in slag mass fraction between 1000 °C and 1200 °C) while the biomass is predicted to be the least slagging (i.e. has the lowest change in mass fraction of slag) in this temperature range. The blends are intermediate to these two extremes, and apart for the 50:50 blend, there is a general trend of them becoming less slagging with increasing biomass; the 50/50 blend is predicted to have a the largest change in slag mass

fraction between 1000 °C and 1200 °C. These general predictions follow the same trend as the slagging index, Fs, (see Eq. (5)) given in Table 5, which is derived from the experimental ash fusion test results.

In the case of pure coal ash, FactSage predicts *ca.* zero slag at 900 °C, 45% slag at 1000 °C (near the experimental SST) and this increases to 90% at 1100 °C (DT is around 1200 °C), so the results are predicting slag at lower temperature than the measured values, but still within about 100 °C. For biomass, significant slag formation is predicted only at 1200 °C and above. Note that the total amount of predicted slag is also much lower for the pine compared to the coal as seen in Fig. 11.

Fig. 11a–c shows the chemical composition of the predicted species calculated using FactSage for the fuels and a 50% mixture
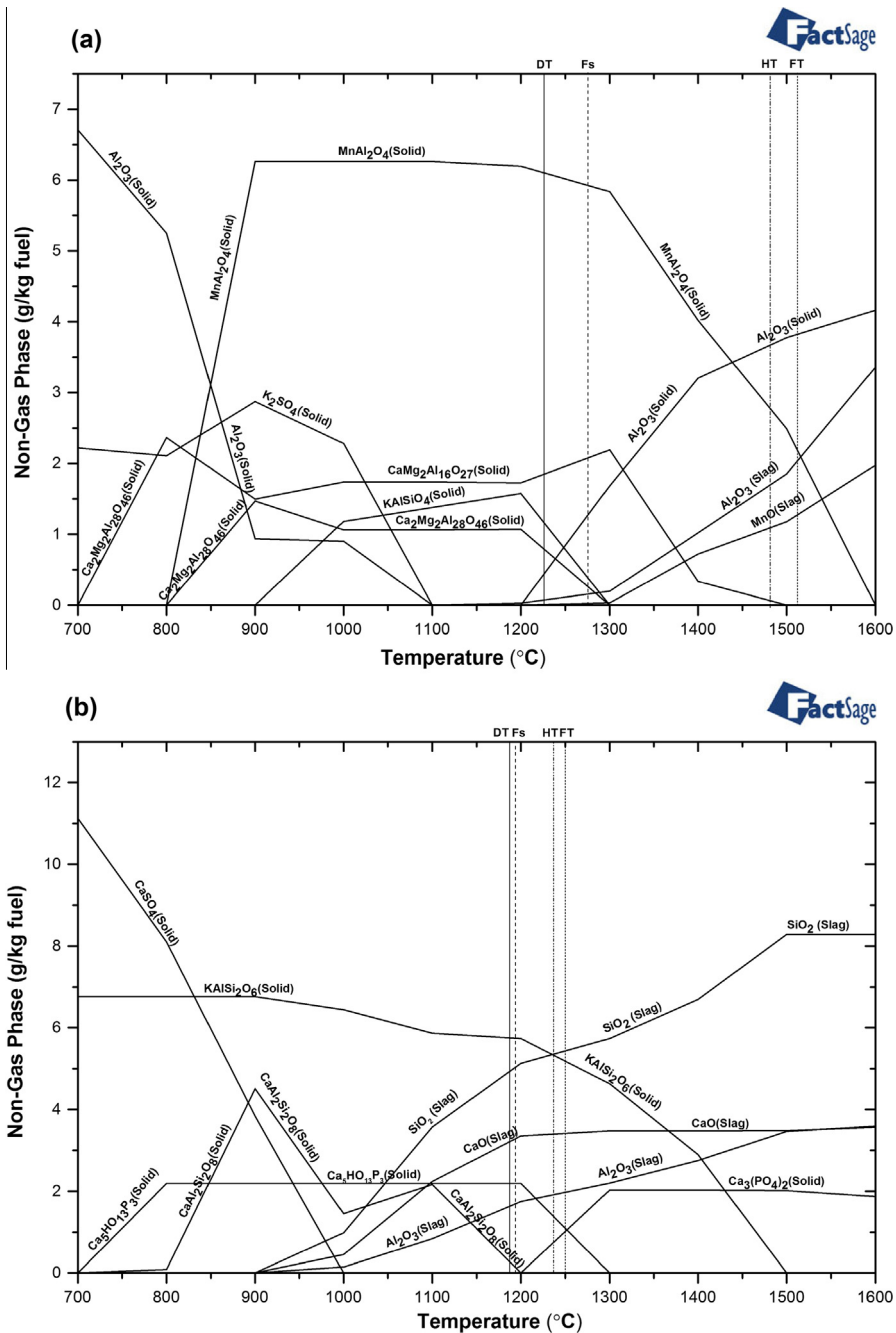

Fig. 11. Stable solid phases in equilibrium with the slag phase for (a) 100% Pine, (b) 50% pine 50% coal, and (c) coal.
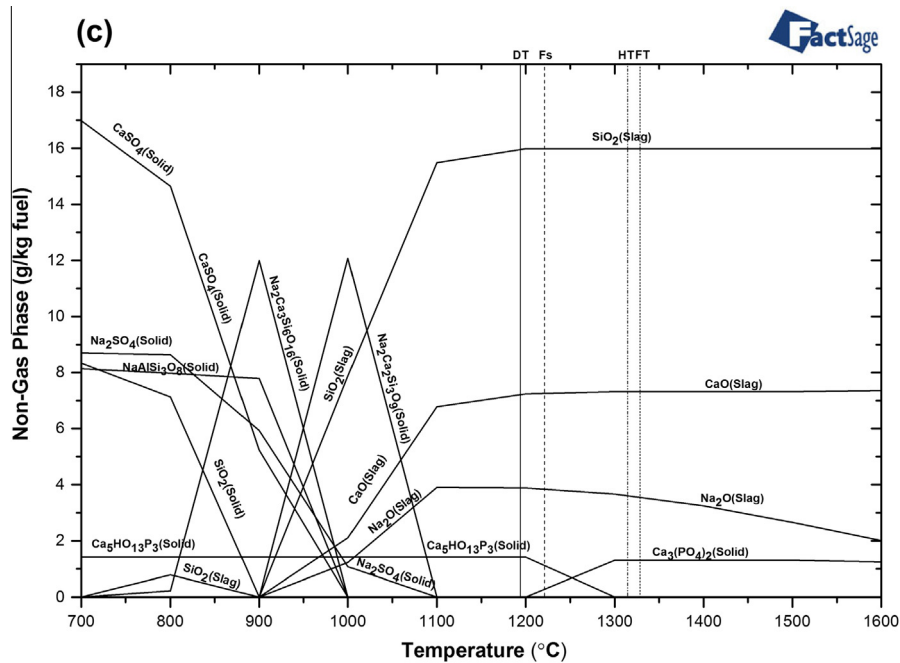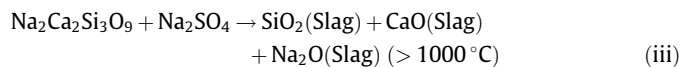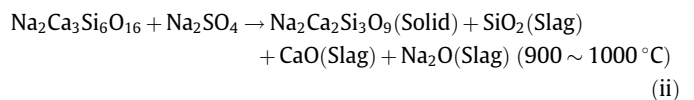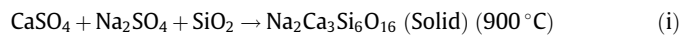
Fig. 11 (*continued*)

of the two. Note that pine, Fig. 11a shows a small propensity of slag formation in terms of g/kg fuel, and this only begins to form at about 1200 °C. In contrast, the coal (Fig. 11c) displays much higher weight of slag and this are first seen to form at above 900 °C. Modelling of the blend (Fig. 11b) predicts intermediate slagging in terms of g/kg fuel, and a small amount of slag is seen at above 900 °C, but this increases significantly at temperatures above 1000 °C. The pine slag is mainly predicted as Al_2O_3, the blend slag as a mixture of SiO_2, Al_2O_3 and CaO and the coal slag as a mixture of SiO_2, CaO, and Na_2O. Compared with the study by Rizvi et al. [17] using a different pine with a lower CaO content than the present work (20 wt% compared with 49 wt%) there are different predicted results for solid phase change and softening temperature.

Comparison of Fig. 11a, Fig. 11b and c shows that the compositions during the phase changes become more complicated. As the coal ratio increases in these three cases the total non-gas phase content increases due to the higher ash content in the fuel. For the solid phase, as the coal ratio increases, Ca mainly exists in $CaSO_4$ and decreases sharply above 700 °C. In the 50/50 mixture below 900C, most of the Ca forms $Ca_5HO_{13}P_3$ and $CaAl_2Si_2O_8$ with a decrease in $CaSO_4$. The Si content increases with an increase in coal ratio, and the higher ash content of coal contributes more Si species in the solid phase. With an increase in temperature $KAlSi_2O_6$ and $CaAl_2Si_2O_8$ in the solid phase are decomposed to SiO_2, CaO and Al_2O_3 which are the main slagging components above 900 °C. Because the amounts of CaO and Al_2O_3 are very close (in Fig. 1), after 1500 °C these two species have similar content in liquid phase. This is also the case in the 50/50 case; in the 100% coal model, $Ca_5HO_{13}P_3$ in the solid phase remains until 1200 °C and changes to $Ca_3(PO_4)_2$ as a solid after 1300 °C. The differences are in the case for 100% coal where most of the K is replaced by Na and combined with Al and Si oxides. As the SiO_2 in the solid phase decreases above 700 °C, SiO_2 occurs for the first time in the slag at 800 °C. After that, because of the decreasing content of $CaSO_4$, Na_2SO_4 and SiO_2 in both solid and liquid phase, these three species react to become $Na_2Ca_3Si_6O_{16}$ as a solid at 900 °C. As the temperature increases, the $Na_2Ca_3Si_6O_{16}$ and $NaAlSi_3O_8$ in the solid phase react to form $Na_2Ca_2Si_3O_9$ as a solid and SiO_2, CaO and Na_2O as slag at 1000 °C. Following that, most $Na_2Ca_2Si_3O_9$

and Na_2SO_4 in solid phase are converted into the liquid phase with significant increase of SiO_2, CaO and Na_2O in the slag. Above 1200 °C, SiO_2 and CaO remain until 1600 °C where some of these species are transferred. The reactions as shown by plots in Fig. 11a–c are

$$CaSO_4 + Na_2SO_4 + SiO_2 \rightarrow Na_2Ca_3Si_6O_{16} \text{ (Solid) } (900\,°C) \qquad \text{(i)}$$

$$Na_2Ca_3Si_6O_{16} + Na_2SO_4 \rightarrow Na_2Ca_2Si_3O_9\text{(Solid)} + SiO_2\text{(Slag)}$$
$$+ CaO\text{(Slag)} + Na_2O\text{(Slag)} \ (900 \sim 1000\,°C) \qquad \text{(ii)}$$

$$Na_2Ca_2Si_3O_9 + Na_2SO_4 \rightarrow SiO_2\text{(Slag)} + CaO\text{(Slag)}$$
$$+ Na_2O\text{(Slag)} \ (> 1000\,°C) \qquad \text{(iii)}$$

3.6. General discussion

The role of laboratory tests of solid pulverised fuels is to simulate their behaviour in an industrial combustor. The fuels were characterised by proximate and ultimate analyses and by the determination of their ash composition. The blends were made principally in two ways, by ashing the blended fuels together (termed 'blended fuel ash') or by ashing separately and blending the ash from each fuel (termed 'ash blends'). There is a clear physical difference between the two ways of producing blends of ashes. In the first case the mixture of fuels will decompose in a way in which the volatiles of each component can interact with each other and this will influence the final composition; the biomass volatiles contain more oxygenated species. Ash produced independently will have already undergone transformations before they are further heated in the blend. However, the temperature of the biomass ashing is too low to result in loss of volatile potassium [36], which is one of the key components which can interact with coal ash in the gas phase [14]. It is debatable, therefore, which method best mimics the behaviour in a large scale combustor where there could be immediate interaction between the two sets of ash especially if some of the ash melts. Nevertheless, experiments produce a consistent finding of unusual slagging behaviour at the 50:50 ash

blend regardless of how the ash is formed, and this behaviour is also modelled in the FactSage calculations.

The data obtained were used to calculate indices to determine the slagging and fouling potential of pine and coal and their blends. From above it is seen that the most appropriate values are calculated from the data for the ash blends. B/A results indicate that pine wood ash has a higher slagging potential than coal ash, which is not bourne out by the ash fusion measurements. Though there are some differences in the predictions of the slagging potential from the different approaches, similar ash melting behaviours were observed by the ash fusion tests and STA-MS experimental methods. Pine ash has a higher shrinkage starting temperature, deformation temperature, hemisphere temperature and flow temperature with a much higher mass loss process than El Cerrejon coal ash. During the STA studies of these two ash blends, it was found that higher percentages of biomass in the fuel bends resulted in decreased slagging propensity. In contrast, the ash fusion temperature (measured in the ash fusion test) was lowest for the 50/50 fuel blend than for any other blend tested here. The fuel ash blends have different fusion temperatures. Shrinkage and/or swelling were also observed during the ash fusion tests. The fusion temperatures and behaviour observed for the different ash samples were replicated by the FactSage model, which resulted in similar phase changes with temperature to the ones observed experimentally.

A further complication comes from comparing the results obtained here with previous published research because of the large difference in the nature of pine samples from different sources as well as the inaccuracies introduced by the widespread use of XRF as an analytical tool, at least in the type of samples studied here.

4. Conclusions

1. Analysis of pine ash and El Cerrejon coal was carried out by both the wet chemical methods and XRF, the former being the most accurate for the type of samples studied here. The accuracy of using the XRF method for pine was not as good as for coal, and equations have been derived to provide corrections for the different components.
2. Measurements were made of the ash fusion temperature characteristics of the fuels and blends. Ash samples of blends were made in two ways, firstly by blending ash produced from the coal and the biomass, and secondly by ashing the blended fuels. Significant differences in the ash fusion temperatures were observed for blends produced by the two methods, whereby ashes from blended fuels had lower characteristic temperatures than blended ashes.
3. Correlations between the hemisphere (HT) and peak endotherm temperatures (STA) showed only limited reliability. For the STA-MS method for studying pyrolysis behaviour the tendencies of mass loss and gas escapes are similar with results from the thermal equilibrium model.
4. Prediction of the pine and coal ash deposition behaviour in different temperature stages can be made by using numerical indices. For the blends, all indices (apart from the empirically-derived slagging index) are unable to replicate fully the ash melting behaviours. It should be noted however, that only one biomass (pine) and coal (El Cerrejon) has been studied, and further work is required to validate this for a waider variety of fuel types. Different methods give different outcomes and so there is a risk of using one method only, and multiple techniques and approaches are advised.
5. Viscosity modelling produced sensible results for the coal and coal/biomass blends, but was not able to replicate the differences observed experimentally from the ash fusion tests. The viscosity models under-predicted the viscosity of the pine ash and how it changes with temperature. The FactSage model performed better than the viscosity model for the coal and the coal:biomass blends and for the pure biomass (pine) ash. The change of gas, solid and liquid phases during pure pine and coal combustion reasonably described the ash deposition behaviour which were also verified by ash fusion tests.

References

[1] Darvell LI, Jones JM, Gudka B, Baxter XC, Saddawi A, Williams A, et al. Combustion properties of some power station biomass fuels. Fuel 2010;89:2881–90.
[2] Niu YQ, Tan HZ, Hui SE. Ash-related issues during biomass combustion: alkali-induced slagging, silicate melt-induced slagging (ash on), agglomeration, corrosion, ash utilization, and related countermeasures. Prog Energy Combust Sci 2016;52:1–61.
[3] Weber R, Mancini M, Mancini NS, Kupka T. On predicting the ash behaviour using Computational Fluid Dynamics. Fuel Process Technol 2013;105:113–28.
[4] Vassilev SV, Baxter D, Andersen LK, Vassileva CG. An overview of the composition and application of biomass ash. Part 1. Phase–mineral and chemical composition and classification. Fuel 2013;105:40–76.
[5] Gudka B, Jones JM, Lea-Langton AR, Williams A, Saddawi A. A review of the mitigation of deposition and emission problems during biomass combustion through washing pre-treatment. J Energy Inst 2015. http://dx.doi.org/10.1016/j.joei.2015.02.007.
[6] Saddawi A, Jones JM, Williams A. Influence of alkali metals on the kinetics of the thermal decomposition of biomass. Fuel Process Technol 2012;104:189–97.
[7] Zhang S, Dong Q, Zhang L, Xiong Y. Effects of water washing and torrefaction on the pyrolysis behaviour and kinetics of rice husk through TGA and Py-GC/MS. Bioresour Technol 2015. http://dx.doi.org/10.1016/j.biortech.2015.08.110.
[8] Carrillo MA, Staggenborg SA, Pineda JA. Washing sorghum biomass with water to improve its quality for combustion. Fuel 2014;116:427–31.
[9] Dayton DC, Jenkins BM, Turn SQ, Bakker RR, Williams RB, Belleoudry D. Release of inorganic constituents from leached biomass during thermal conversion. Energy Fuels 1999;13:860–70.
[10] Wieland C, Kreutzkam B, Balan G, Spliethoff H. Evaluation, comparison and validation of deposition criteria for numerical simulation of slagging. Appl Energy 2012;93:184–92.
[11] López IC, Ward CR. Composition and mode of occurrence of mineral matter in some Colombian coals. Int J Coal Geol 2008;73:3–18.
[12] Wang G, Pinto T, Costa M. Investigation on ash deposit formation during the co-firing of coal with agricultural residues in a large-scale laboratory furnace. Fuel 2014;117:269–77.
[13] Wang G, Silva RB, Azevedo JLT, Martins-Dias S, Costa M. Evaluation of the combustion behaviour and ash characteristics of biomass waste derived fuels, pine and coal in a drop tube furnace. Fuel 2014;117:809–24.
[14] Bryers RW. Fireside slagging, fouling and high-temperature corrosion of heat-transfer surface due to impurities in steam-raising fuels. Prog Energy Combust Sci 1996;22:29–130.
[15] Hao W, Bashir WMS, Jensen PA, Sander B, Glarborg P. Impact of coal fly ash addition on ash transformation and deposition in a full-scale wood suspension-firing boiler. Fuel 2013;113:632–43.
[16] Baxter XC, Darvell LI, Jones JM, Barraclough T, Yates NE, Shield I. Study of Miscanthus × giganteus ash composition – variation with agronomy and assessment method. Fuel 2012;95:50–62.
[17] Rizvi T, Xing P, Pourkashanian M, Darvell LI, Jones JM, Nimmo W. Prediction of biomass ash fusion behaviour by the use of detailed characterisation methods coupled with thermodynamic analysis. Fuel 2015;141:275–84.
[18] Xu J, Yu GS, Liu X, Zhao F, Chen XL, Wang FC. Investigation on the high-temperature flow behaviour of biomass and coal blended ash. Bioresour Technol 2014;166:494–9.
[19] Reinmoller M, Klinger M, Schreiner M, Gutte H. Relationship between ash fusion temperatures of ashes from hard coal, brown coal, and biomass and mineral phases under different atmospheres: a combined FactSage^{TM} computational and network theoretical approach. Fuel 2015;151:118–23.
[20] Friedl A, Padouvas E, Rotter H, Varmuza K. Prediction of heating values of biomass fuel from elemental composition. Anal Chim Acta 2005;544:191–8.

[21] Majumder AK, Jain R, Banerjee P, Barnwal JP. Development of a new proximate analysis based correlation to predict calorific value of coal. Fuel 2008;87:3077–308.
[22] Jenkins BM, Baxter LL, Miles JTR, Miles TR. Combustion properties of biomass. Fuel Process Technol 1998;54:17–46.
[23] Lawrence A, Kumar R, Nandakumar K, Narayanan K. A novel tool for assessing slagging propensity of coals in PF boiler. Fuel 2008;87:946–50.
[24] Li QH, Zhang YG, Meng AH, Li L, Li GX. Study on ash fusion temperature using original and simulated biomass ashes. Fuel Process Technol 2013;107:107–12.
[25] McLennen AR, Bryant GW, Bailey CW, Stanmore BR, Wall TF. Index for iron based slagging for pulverized coal firing in oxidizing and reducing conditions. Energy Fuel 2000;14:349–54.
[26] Watt JD, Fereday F. The flow properties of slag formed from the ashes of British coals: Part 1: viscosity of homogeneous liquid slag in relation to slag composition. J Inst Fuel 1969;42:99–103.
[27] Vargas S, Frandsen FJ, Dam-Johansen K. Rheological properties of high–temperature melts of coal ashes and other silicates. Progr Energy Combust Sci 2001;27:237–429 [and references therein].
[28] Degereji MU, Ingham DB, Ma L, Pourkashanian M, Williams A. Numerical assessment of coals/blends slagging potential in pulverized coal boilers. Fuel 2012;102:345–53.
[29] Degereji MU, Gubba SR, Ingham DB, Ma L, Pourkashanian M, Williams A, et al. Predicting the slagging potential of co-fired coal with sewage sludge and wood biomass. Fuel 2013;108:550–6.
[30] www.factsage.com.
[31] Kong LX, Bai J, Li W, Wen XD, Liu XC, Li XM, et al. The internal and external factor on coal ash slag viscosity at high temperatures, Part 2: effect of residual carbon on slag viscosity. Fuel 2015;158:976–82.
[32] Nordgren D, Hedman H, Padban N, Boström D, Öhman M. Ash transformations in pulverised fuel co-combustion of straw and woody biomass. Fuel Process Technol 2013;105:52–8.
[33] Du S, Yang H, Qian K, Wang X, Chen H. Fusion and transformation properties of the inorganic components in biomass ash. Fuel 2014;117:1281–7.
[34] Thyrel M, Samuelsson R, Finell M, Lestander TA. Critical ash elements in biorefinery feedstock determined by X-ray spectroscopy. Appl Energy 2013;102:1288–94.
[35] Pang CH, Hewakandamby B, Wu T, Lester E. An automated ash fusion test for characterisation of the behaviour of ashes from biomass and coal at elevated temperatures. Fuel 2013;103:454–66.
[36] Mason PE, Darvel LI, Jones JM, Williams A. Potassium release patterns during combustion of single particles of biomass. P Combust Inst 2016. http://dx.doi.org/10.1016/j.proci.2016.06.020.